Annexure -III

UNIVERSITY GRANTS COMMISSION
BAHADUR SHAH ZAFAR MARG
NEW DELHI – 110 002.

Final Report of the work done on the Major/Minor Research Project. (Report to be submitted within 6 weeks after completion of each year).

1. Project report No. 1st /2nd /3rd /Final : Final

2. UGC Reference No.: F.No. 37-188/ 2009 (SR), dated 12.1.2010

3. Period of report: from 1.2.2010 to 31.1.2013

4. Title of research project : "Molecular modification of Pyrimidinones: Potential Antiviral agents"

5. (a) Name of the Principal Investigator: Dr. Kamaljit Singh

(b) Deptt. and University/College where work has progressed

Department of Applied Chemical Sciences and Technology, Guru Nanak Dev University, Amritsar

6. Effective date of starting of the project: 1.2. 2010

7. Grant approved and expenditure incurred during the period of the report:

a. Total amount approved Rs. 8,44,800/- (Grant received: 5,95,040/-)

b. Total expenditure Rs. 5,39,040/-

Report of the work done: (Please attach a separate sheet)

(i) Brief objective of the project :

1. To undertake synthetic manipulations at 1-, 2-, 3-, 5- and/or 6-positions and unambiguous characterisation ofth eproducts.
2. Molecular modelling, docking experiments and evaluation of compounds for anti HIV, antiviral, cardioregulatory as well as antiinflammatory activities.
3. To draw structure-activity correlations and to design potent drug entities.

iii. Work done so far and results achieved and publications, if any, resulting from the work (Give details of the papers and names of the journals in which it has been published or accepted for publication

Work done in the project:

(A-1) A facile transformation of Biginelli pyrimidin-2(1H)-ones to pyrimidines. In vitro evaluation as inhibitors of Mycobacterium tuberculosis and modulators of cytostatic activity

A series of pyrimidine derivatives bearing amine substituents at C-2 position were obtained from Biginelli 3,4-dihydropyrimidin-2(1*H*)-ones and the effect of structural variation on anti-tuberculosis (anti-TB) activity against *Mycobacterium tuberculosis* $H_{37}RV$ strain and antiviral activity in a series of cell cultures has been evaluated. While the compounds were found to possess structure dependent cytostatic activity, these were not found to be efficient inhibitors of *Mycobacterium tuberculosis* nor did they inhibit a broad variety of DNA or RNA viruses in cell culture.

To meet the above objectives, we have reported a straight forward conversion of Biginelli dihydropyrimidinones **1** (DHPMs)[1] into C-2 amine substituted pyrimidine derivatives **4** as shown in Scheme 1. Oxidation of DHPM derivatives **1** (Scheme 1) to 1,2-dihydropyrimidin-2-one derivatives **2** was readily achieved using pyridinium chlorochromate (PCC).[2] Subsequent treatment of appropriate **2** with phosphorous

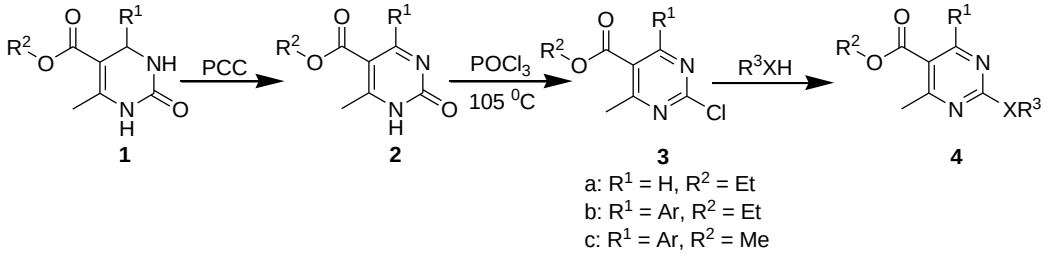

Scheme 1. Synthesis of 2-substituted pyrimidine-5-carboxylate **4** derivatives.

oxychloride at 105^{o}C furnished corresponding 2-chloro derivatives **3a-c**,in 85%, 91% and 93% yield, respectively. Further reaction of **3a-c** with N- and O-nucleophiles, furnished corresponding 2-substituted pyrimidine derivatives **4**,in very good yields (68-97%). This fairly simple and efficacious protocol can be visualized as a general protocol for obtaining a range of C-2 substituted pyrimidine analogues, for obtaining C-2 diversified pyrimidine derivatives.

The minimum inhibitory concentration (MIC) values are reported in Table 1, it has been deduced that the presence of a *N*-benzyl group at C-2 position (**4d**) or better a 3-aminoaniline substituent(**4l**) seems to be useful for significant antitubercular activity. The presence of an ethyl ester, rather than methyl ester substituent at C-5 position of the pyrimidine core (**4d** vs **4e**) led to improvement in MIC values. Replacing the 3-aminoaniline substituent in **4l** with 2-hydroxyaniline, piperidine or morpholine substituent at C-2 position to form **4j**, **4m** and **4n**, respectively, only raised the MIC, without a significant effect on % inhibition. Replacing 3-hydroxypropyl amine substituent from C-2 position of **4f** with *n*-propylamino substituent (**4h**) saw both an increase in % inhibition as well as marginal decrease in MIC. However, none of these derivatives were found to be significantly active.

Table 1. The structure and anti-TB activity (MIC) against *Mycobacterium tuberculosis* for selected pyrimidine-5-carboxylate **4** derivatives.

Compound	% inhibition at 128 μM	MIC (μM)
4d	93	63.8
4e	3	> 128
4f	57	> 128
4h	99	117.7
4j	92	121.8
4l	99	31.2
4m	86	> 128
4n	96	125.3
Isoniazid	-	0.12
Moxifloxacin	-	0.47
PA-824	-	0.48

While screening pyrimidine derivatives for their activity against a broad variety of DNA and RNA viruses (including HIV) in the appropriate cell culture models, we observed that while none of the C-2 alkyl/aryl/amine substituted dihydropyrimidinone derivatives showed appreciable activity against any of the investigated viruses at subtoxic concentrations, C-2 amine substituted pyrimidine derivatives **4e** and **4d** proved markedly cytostatic against MDCK cell cultures (IC_{50}: 0.9 μg/mL and 1.2 μg/mL, respectively). Compound **4e** was more cytotoxic (MCC: 4-10 μg/mL) to confluent cell cultures (i.e., human embryonic lung cells, feline Crandell kidney cells) than **4d** (MCC: ≥100 mg/mL) in these cell cultures. Therefore, representative members of the newly synthesized compounds **4** were evaluated for their inhibitory effect against the proliferation of murine leukemia (L1210), murine mammary carcinoma (FM3A), human T-lymphocyte (CEM), and human cervix carcinoma (HeLa) cells (Table 2). Whereas, pyrimidine derivatives bearing amino (**4a-c**, **4f-h**), morpholino (**4n**) and ethoxy (**4o**) substituents at the C-2 position (Table 1) depicted a marginal cytostatic activity of the test compounds (IC_{50}: 86-500 μM), more bulky aryl group containing derivatives such as **4i-l**, bearing groups such as tryptamine (**4i**), 2-hydroxyaniline (**4j**), 4-hydroxyaniline (**4k**) and 2-aminoaniline (**4l**) rendered a significantly higher antiproliferative activity (IC_{50}: 13-58 μM) (Table 2). The C-2 piperidine substituted pyrimidine derivative **4m** also showed higher cytostatic activity. 4-Hydroxyanilne substituted pyrimidine derivative **4k** showed highest cytostatic activity (IC_{50}: 13 μM) against CEM cells.

Table 2. Inhibitory effect against the proliferation of murine leukemia (L1210), murine mammary carcinoma (FM3A), human T-lymphocyte (CEM) and human cervix carcinoma (HeLa) cells.

	IC_{50}[a](μM)			
Compound	L1210	FM3A	CEM	HeLa
4a	245 ± 34	432 ± 96	207 ± 45	183 ± 23
4b	402 ± 139	336 ± 177	382 ± 166	216 ± 29
4c	378 ± 83	306 ± 6	480 ± 29	147 ± 13
4f	238 ± 9	213 ± 0	150 ± 33	213 ± 14
4g	132 ± 28	174 ± 2	118 ± 44	86 ± 45
4h	164 ± 13	192 ± 12	162 ± 40	138 ± 2
4i	28 ± 6	34 ± 4	31 ± 3	23 ± 9
4j	58 ± 4	52 ± 4	43 ± 3	50 ± 11
4k	24 ± 9	24 ± 2	13 ± 4	24 ± 5
4l	46 ± 3	43 ± 1	46 ± 8	50 ± 2
4m	43 ± 2	55 ± 1	72 ± 41	47 ± 3
4n	> 500	> 500	≥ 500	≥ 500
4o	251 ± 45	239 ± 54	120 ± 66	135 ± 71

(A-2) 2-Aminopyrimidine based 4-aminoquinoline anti-plasmodial agents.

We envisaged that linking 7-chloro-4-aminoquinoline unit, critical for antimalarial activity through a diversely functionalized lateral side chain with other antimalarial moiety such as aminopyrimidine, might furnish *conjugate hybrids* capable of showing useful antimalarial activity. Thus, 2-aminopyrimidine based 4-aminoquinolines were synthesized using an efficacious protocol. Some of the compounds showed *in vitro* antiplasmodial activity against drug-sensitive CQ^S (3D7) and drug-resistant CQ^R (K1) strains of *P. falciparum* in the nM range. In particular, 5-isopropyloxycarbonyl-6-methyl-4-(2-nitrophenyl)-2-[(7-chloroquinolin-4-ylamino)butylamino] pyrimidine depicted the lowest IC_{50} (3.6 nM) value (56-fold less than CQ) against CQ^R strain. Structure-activity profile and binding with heme, μ-oxo-heme have been studied.[3-7] Binding assays with DNA revealed better binding with target parasite type AT rich pUC18 DNA. Most compounds were somewhat cytotoxic, but especially cytostatic. Molecular docking analysis with *Pf* DHFR allowed identification of stabilizing interactions.

Compounds **10a-s** were synthesized as outlined in Scheme 2, *via* a common intermediate **8**. 3,4-Dihydropyrimidin-2(1*H*)-ones **6** were prepared through HCl-catalyzed Biginelli condensation of appropriate aldehyde (R^3CHO), alkylacetoacetate

($R^2CH_2COOR^1$) and urea.[1] Dehydrogenation of **6** using pyridinium chlorochromate **5** in DCM furnished pyrimidinones **7**.[2] Refluxing **7** with $POCl_3$ yielded **8** which upon nucleophilic substitution reaction with appropriate 4-amino-7-chloroquinoline **9** gave **10a-s** in a synthetically useful manner.

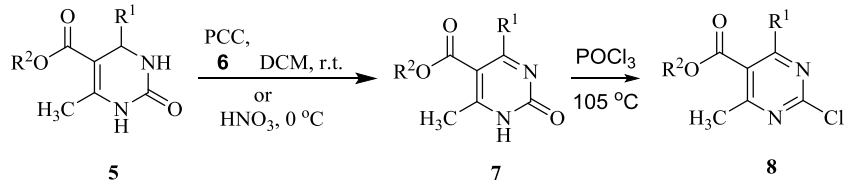

5 **7** **8**

a: $R^1 = C_6H_5$, $R^2 = C_2H_5$; b: $R^1 = CH_3$, $R^2 = C_2H_5$; c: $R^1 = 2\text{-}NO_2C_6H_4$, $R^2 = CH(CH_3)_2$; d: $R^1 = 3\text{-}NO_2C_6H_4$, $R^2 = CH(CH_3)_2$; e: $R^1 = 4\text{-}NO_2C_6H_4$, $R^2 = CH(CH_3)_2$; f: $R^1 = C_6H_5$, $R^2 = CH_3$; g: $R^1 = C_6H_5$, $R^2 = CH(CH_3)_2$; h: $R^1 = CH_3$, $R^2 = CH_3$; i: $R^1 = 4\text{-}ClC_6H_4$, $R^2 = C_2H_5$; j: $R^1 = 4\text{-}FC_6H_4$, $R^2 = C_2H_5$; k: $R^1 = 2\text{-}NO_2C_6H_4$, $R^2 = C_2H_5$; l: $R^1 = H$, $R^2 = C_2H_5$

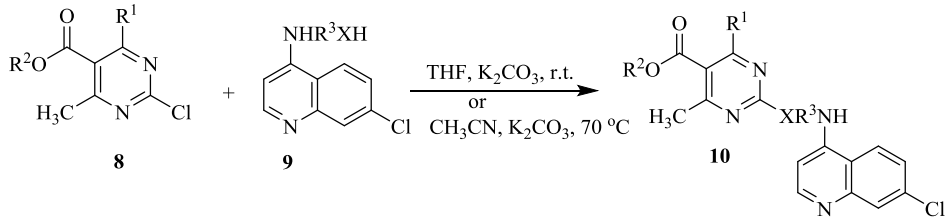

8 **9** **10**

Scheme 2. Synthesis of 2-aminopyrimidine based 4-aminoquinolines **10**.

The *in vitro* antiplasmodial activities of **10a-s** were determined in primary and secondary screening against CQ^S and CQ^R strains of *P. falciparum.* The half maximal inhibitory concentration (IC_{50}) of **10a-s** are summarised in Table 3. Evidently, the compounds have antiplasmodial activity in the nM range and against the CQ^R strain of *P. falciparum,* in some cases activity was found to be even superior to CQ. Systematic variation of the length as well as nature of the spacer connecting the pharmacophores discerned useful trends in the antiplasmodial activity of these analogues.

The better antiplasmodial activity of phenyl-substituted pyrimidine compounds against the CQ^R strain may be attributed to optimal fitting of these compounds in the active site of *Pf*DHFR leading to a favourable conformation for π-π interaction with the heme functionality. Moreover, the introduction of a nitro substituent on the phenyl ring at the C-4 position of the pyrimidine core results in a significant increase in antiplasmodial activity as well as resistance against the CQ^R strain, although it has little effect on activities against the CQ^S strain (Table 3). Also, the corresponding *o*-, *m*- or *p*-nitro derivatives showed considerable variation in antiplasmodial activity (Table 3).

Comparison of compounds (**10n**, **10q**, **10s**) having an identical spacer reveals that the *p*-NO_2 substituted **10s** (IC_{50} 175.8 nM) is more active than the *o*-/*m*-NO_2 substituted compounds **10q** and **10n**, respectively, but are less active than the unsubstituted ethyl ester analogue **10b**. Further, comparison with the butyl spacer analogue suggests that *o*-NO_2 phenyl derivative **10r** is more potent than the *m*-NO_2 counterpart **10o**, as well as its ethyl ester analogue **10c**, against the CQ^R strain. Compound **10r** was found to be the most active compound in this series against the CQ^R strain with antiplasmodial activity (IC_{50} 3.6 nM), 56 times more than CQ (IC_{50} 201.8 nM) and comparable to artesunate (IC_{50} 2.8 nM) (Table 3).

These findings could be attributed to the increased steric bulk (**10h** more than **10i**) affecting the interaction of the iron centre of heme with the compounds. This has been corroborated by performing the titration of monomeric heme with both **10h** and **10i**. While the titration of heme (2.4 µM, DMSO:H_2O/ 4:6, v/v) with increasing concentration of **10h** (0-85.7 µM, DMSO:H_2O/4:6, v/v) revealed no change in the absorbance at 402 nm (Figure 1a), the addition of **10i**, in a similar way showed marked gradual decrease in absorbance at 402 nm. The decrease in absorbance continued until the concentration of **10i** was 8.85 µM (Figure 1b), representing 1:4 molar ratio of heme and **10i**. Hence, the flexibility, chain length and steric constraints of the spacer linking quinoline moiety and pyrimidine unit seem to play a role in antiplasmodial activity of these derivatives. Although the *in vitro* activity of **10a-c**, **10p** and especially **10r** (IC_{50} 3.6 nM) was superior to CQ (IC_{50} 201.8 nM) against the CQ^R strain, these compounds suffer from high ClogP values (Table 3), which are suggestive of the fact that these possess limited aqueous solubility, which in fact is not a serious limitation in view of recent advancements in formulation methods.

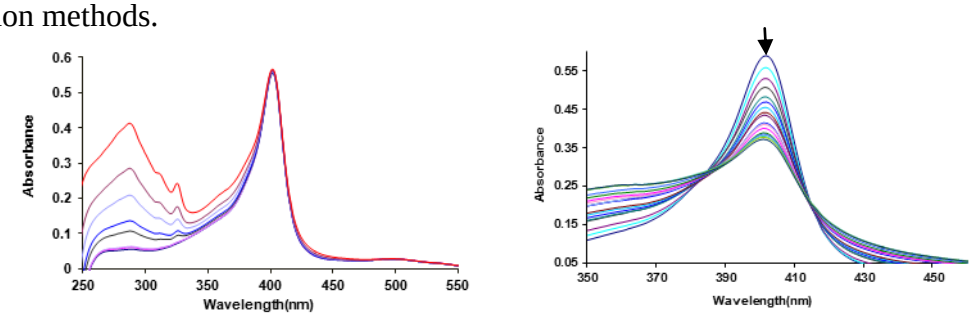

Figure 1. Titration of **10h** (0-85.7 µM, DMSO: H_2O/4:6, v/v) (a) and **10i** (0-8.85 µM, DMSO:H_2O/4:6, v/v)(b) with heme (2.4 µM, DMSO: H_2O/ 4:6, v/v).

Antiviral activity of the compounds **10a-c**,**10l-n**,**10p** and**10r**, which were active against the CQ^R strain was also evaluated against (i) parainfluenza-3 virus, reovirus-1, Sindbis virus, Coxsackie virus B4, Punta Toro virus in vero cell cultures, (ii) herpes simplex virus -1 (HSV-1; KOS), herpes simplex virus-2 (HSV-2; G), vaccinia virus, vesicular stomatitis virus, herpes simplex virus-1 (TK^-KOS ACV^R), cytomegalovirus, varicella-zoster virus in HEL cell cultures, (iii) vesicular stomatitis virus, coxsackie virus B4, respiratory syncytial virus in HeLa cell cultures, (iv) influenza A virus (H1N1 and H3N2) and influenza B virus in MDCK cell cultures and (v) feline corona virus (FIPV) and feline herpes virus activity in CRFK cell cultures. Unfortunately, no significant antiviral activity was noted at subtoxic concentrations. Most compounds were somewhat cytotoxic to the different cell lines (confluent non-proliferating cultures), but especially cytostatic against proliferating (Vero/MDCK/ CRFK) cell cultures. Chloroquine has been shown to inhibit HIV through blockade of viral entry *via* inhibition of endosomal acidification.[8-9]Compounds **10a-c**, **l-n**, **p**, **r** were also tested against HIV-1 as well as HIV-2 in human T-lymphocyte (CEM) cell cultures. However, none of the compounds were active at subtoxic concentrations.

Generally, the compounds exhibit a relatively high cytostatic activity but displayed a fairly safe selectivity index (except **10m** and **10n**) in the range of 10.04 to 638 against MDCK cell cultures. The most active compound **10r** with an IC_{50} value of 3.6 nM against CQ^R strain exhibited a highest selectivity index (SI = 638), **10l** with an IC_{50} value of 160.8 nM against CQ^R strain exhibited a high selectivity index (361.9). However, **10m** having an IC_{50} value of 1659.8 nM was most toxic with a selectivity index of 0.48.

The plausible mechanism of *in vitro*antiplasmodial action against CQ^R strain has been investigated for **10c** and **10r**, found to be most potent of the series of the compounds reported herein IC_{50} 26.1 nM, **10c** and IC_{50} 3.6 nM, **10r**). These compounds are also expected to bind to heme [Fe(III)PPIX] (hydroxo or aqua complex of ferriprotoporphyrin IX) in solution and inhibit aggregation to β-hematin, in much the same way as CQ itself. The association constant of **10c** is found to be greater (log *K* 6.018) than **10r** (log *K* 5.078). Decrease in the apparent pH from 7.5 to 5.6 caused a fairly modest decrease in

log *K* values of both **10c** and **10r**, indicating a strong binding to heme even at acidic pH.

The binding of **10c** and **10r** was also assessed from their ^{1}H NMR titration with heme.

Table 3. Yield, *In vitro* antiplasmodial activity,cytotoxicity, resistance factor and selectivity index of compounds **10a-s**.

Compound (% yield)	IC_{50} (nM)		Resistance factor[e]	ClogP[f]	Cytotoxicity (μM)[g]		Selectivity index[j]
	CQ^S (3D7)[a,b]	CQ^R (K1)[c,d]			CC_{50}[h]	MIC[i]	
10a (89)	21.7	139.3	6.43	6.83	1.4	0.8	10.04
10b (84)	247.5	52.2	0.210	6.82	0.8	0.8	15.33
10c (77)	202.3	26.1	0.129	7.35	0.9	0.8	34.41
10d(67)	1134.9	617.7[b]	0.544	8.94	-	-	-
10e (72)	252.2	516.4	2.047	9.47	-	-	-
10f (64)	1776.8	487.7	0.2744	10.53	-	-	-
10g (65)	264.8	853.7	3.22	11.58	-	-	-
10h (53)	14828.3	27320.9	1.842	8.81	-	-	-
10i(57)	644.4	6186.4[b]	9.600	8.80	-	-	-
10j (58)	15888.5	28096.7	1.7683	5.31	-	-	-
10k(55)	286.7	860.4[b]	3.00	8.28	-	-	-
10l (92)	63.1	160.8	2.5480	5.64	58.2	20	361.89
10m(90)	42.1	1659.8[b]	39.422	5.75	0.8	4	0.48
10n(71)	598.7	230.5[b]	0.385	7.30	0.5	0.8	2.1
10o (78)	697.2	192.1	0.2756	7.30	-	-	-
10p (66)	172.9	96.0	0.5555	6.89	2.2	≥0.8	22.90
10q (73)	1955.1	229.3	0.1173	7.30	-	-	-
10r (85)	18.2	3.6	0.2	7.30	2.3	4.0	638
10s (82)	499.9	175.8	0.3518	7.30	-	-	-
Artesunate	5.3	2.8	0.5418	1.06	-	-	-

[a]CQ sensitive strain; [b]primary screening; [c]CQ resistant strain; [d]secondary screening; [e]calculated by dividing IC_{50} values of PFK1 by PF3D7; [f]calculated from Chem draw Ultra 11.0; [g]determined onMadin Darby canine kidney (MDCK)cells; [h]50% cytotoxic concentration, as determined by measuring the cell viability with the colorimetric formazan- based MTS assay (reference drugs used: Oseltamivir carboxylate CC_{50}/MIC >100, Ribavirin CC_{50}/MIC >100, Amantadine CC_{50}/MIC >200 and Rimantadine CC_{50}/MIC >200); [i]minimum compound concentration that causes a microscopically detectable alteration of normal cell morphology; [j]Selectivity Index(S.I.) is calculated as CC_{50}/ IC_{50}(K1 Strain) ratio.

Table 4. β-Hematin inhibitory assay.

Compound	% Inhibition[a]	Compound	% Inhibition[a]
10a	96	10l	66
10b	100	10m	100
10c	100	10n	79
10d	89	10o	92
10e	56	10p	-
10f	-	10q	89
10g	-	10r	100 (2)[b]
10h	53	10s	94
10i	100	CQ	18 [b]
10j	35	Quinine	324[b]
10k	-		

[a]*The percentage inhibition at 1mg/ml (highest concentration tested);* [b]IC_{50} *(μM).*

As shown in Table 4, there is a general correlation between antiplasmodial activity and inhibition of β-hematin formation, but the same generalisation does not hold for compound **10h**, as, in spite ofhaving 100% β-hematin inhibition, it is one of the least active (IC_{50}27320.9 nM, CQ^R and IC_{50} 14828.3 nM, CQ^S) compounds of the series.

We have also investigated the binding of the most active of the series, **10c** and **10r** towards GC rich Calf Thymus DNA (CT DNA) as well as AT rich pUC18 DNA through stepwise addition of small increments of DNA to a solution the compounds at constant concentration as well as physiological pH (Figure 2A & 2B). A progressive decrease in the characteristic quinoline ring absorptions at 320 and 340 nm attributable to the intercalation of the quinoline into DNA was indicated.

A

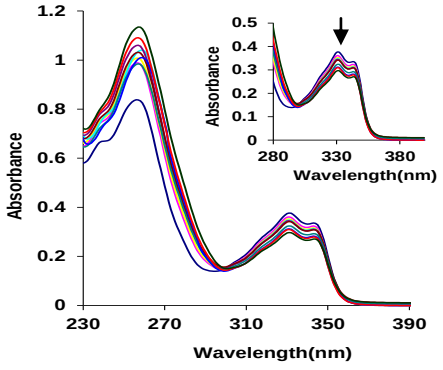

B

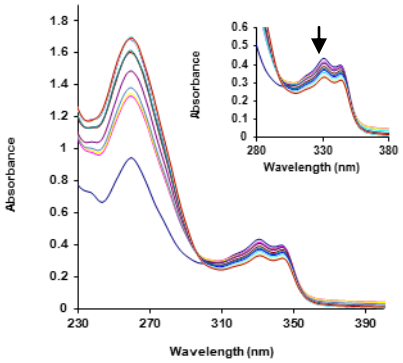

Figure 2. Absorption spectra of **10c** (A) and **10r** (B) in the presence of different CT DNA concentration inset show zoom between 280 and 380 nm.

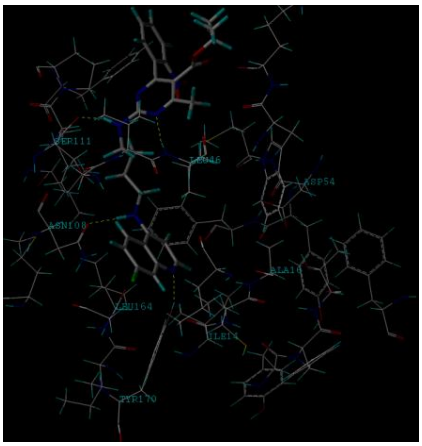

Figure 3. The interactions of the substrate **10r** in the active site cavity of the enzyme *Pf* DHFR. The hydrogen bonding interactions with the amino acids Ile14, Leu46, Asn108, Ser111 and Try170 are shown with dotted yellow lines.

Figure 3 shows the top scoring binding pose of **10r** in the active site of *Pf* DHFR. The docking score for **10r** is -24.5, which is much better than that of the lead compound **5** (-20.1). The origin of this improvement in docking score can be traced to the increased number of stabilizing interactions between **10r** and *Pf* DHFR, in comparison to the interactions between **5** and *Pf* DHFR. **10r** shows hydrogen bonding interaction with Tyr170 and Asn108 residues; these two interactions are common to **10r** as well as to **5**. In addition, **10r** shows hydrogen bonding interaction with Ser111 and Leu46 residues. These additional stabilizing interactions ensure that **10r** adopts a slightly different (and improved) pose in comparison to that of **5**. These improved interactions can be considered as deterministic factors for the improved anti-plasmodial activity of **10r**.

Publications from this work:

1. Kamaljit Singh, Hardeep Kaur, Kelly Chibale, Jan Balzarini, Susan Little, Prasad V. Bharatam, *Eur. J. Med. Chem*., **2012**, 52, 82-97.
2. Kawaljit Singh and Kamaljit Singh, Biginelli condensation: Synthesis and structure diversification of 3,4-dihydropyrimidin-2(1H)-one derivatives. Chapter 3 in *Adv. Het. Chem.* (AR Katritzky Ed.), **2012**, 105, 224-288.
3. Kamaljit Singh, Kawaljit Singh, Baojie Wan, Scott Franzblau, Kelly Chibale, Jan Balzarini, *Eur. J. Med. Chem*., **2011**, 46, 2290-2294.
4. Kamaljit Singh, Kawaljit Singh and Hardeep Kaur, *Tetrahedron*, **2012,** 68, 6169-6176.

(A 3) A quinoline-pyrimidine based turn-off fluorescent cation sensor

Sensing of analytes is an active area of research in coordination and supramolecular chemistry, driven by the vast potential for industrial, environmental and biological applications. Several methods, such as high-performance liquid chromatography, mass spectrometry, atomic absorption spectroscopy, inductively-coupled plasma atomic emission spectrometry, electrochemical sensing etc. have been developed to analyze the target analytes.[10]

The detection and control of analytes comprising of cations, anions and neutral molecules has become an indispensable task in many activities related to the management of minimum standards of edible products, environment, agriculture sciences, medicine and health sciences.[11] The stringent requirements imposed by regulating agencies have led to the development of suitable sensors capable of sensing and controlling different analytes. Consequently, the search for the compounds whose properties are modified in the presence of a target analyte is a matter of great practical significance. One of the important ways to sense analytes is through the use of chemosensors, in particular those exhibiting optical response, either absorption and/or emission. Effective operational usage of these chemosensors requires their high sensitivity and selectivity towards the analytes. Although a large variety of highly selective[12] single as well as multianalyte chemosensors[13] have been reported, the development of sensors for multianalyte

detection in real time is still a challenge. The use of fluorescence as the signal transducing method in optical sensors offers distinct advantages in terms of sensitivity, selectivity and response time.[14] Consequently, fluorescent molecular sensors have attracted considerable recent interest.[15]

Keeping this in view, we evaluated the cation and anion binding properties of quinoline -pyrimidine hybrid **10c.** Receptor **10c** which was synthesized by following the steps described in Scheme 2, shows turn-off fluorescent behavior in the presence of Hg^{2+}, Fe^{3+} and Cu^{2+} over other cations and offers discrimination of these cations from each other on the basis of the extent of quenching.

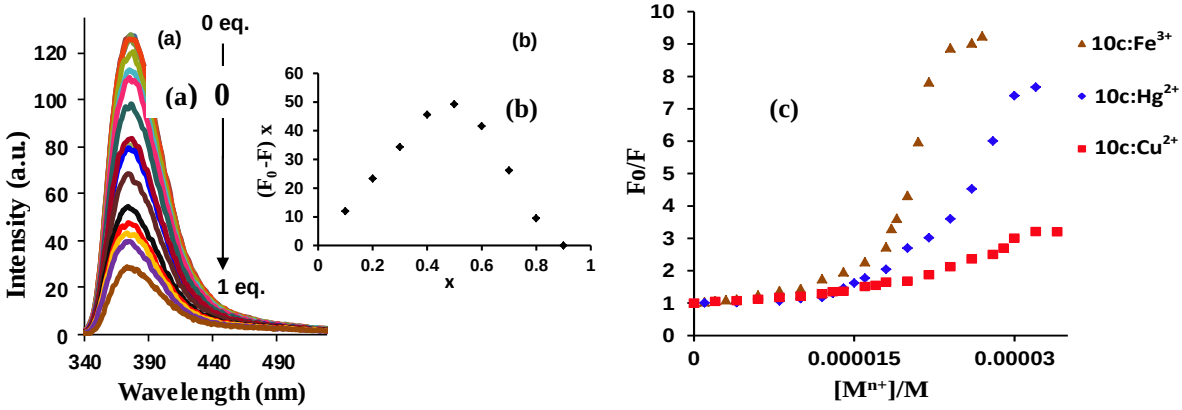

Figure 4 (a) Fluorescence spectra of **10c** (30 μM) in CH_3OH upon addition of Hg^{2+} (0-1.0 equiv.) in distilled H_2O (λ_{ex} = 330 nm) at pH 7.4; (b) Job plot of Hg^{2+} complex formation. x = [**10c**]/[**10c**]+[Hg^{2+}] is the mole fraction of the **10c**, F_0 is the fluorescence intensity when x = 1 and F is the fluorescence intensity at respective values of x; (c) Stern-Volmer plots for M^{n+}, where M^{n+} = Fe^{3+}, Hg^{2+}, and Cu^{2+}.

The fluorescence emission spectrum (λ_{ex} = 330 nm) of **10c** (30 μM in CH_3OH) exhibits an emission band at 376 nm. The calculated quantum yield is 0.024 which is relatively low compared to the usual values. The incremental addition of Hg^{2+}, Fe^{3+} and Cu^{2+} solutions (0–1.0 equiv. in distilled H_2O) caused 69–94% quenching of the emission which was stabilized when the addition of 1 equiv. of the cation was achieved (Fig. 4 a).

Furthermore, a Job plot suggested 1: 1 stoichiometry where the maximum emission change was observed when the mole fraction of **10c** versus the cation was 0.5 in each case (Fig. 4b). Stern–Volmer plots were created for the titration of these cations (Fig. 4c). The non-linear nature of the Stern–Volmer plot with an upward curvature (Fig.

4c) indicates the possible involvement of combined dynamic and static quenching. However, it is interesting to note that the degree of quenching is large for Fe^{3+} followed by Hg^{2+} and lower for Cu^{2+}, which is important for discriminating these cations from each other (Fig. 4c).

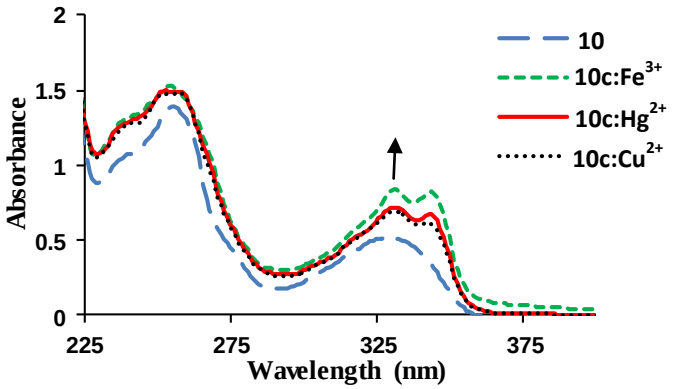

Figure 5. Changes in the UV-vis absorption spectra of **10c** (30 μM) in CH_3OH and its complexes with Fe^{3+} (32 μM), Hg^{2+} (35 μM) and Cu^{2+} (40 μM) in distilled H_2O at pH 7.4.

The UV-vis absorption spectrum of **10c** exhibited bands at 330 nm (ε_{max} 15 733 L mol^{-1} cm^{-1}) and 255 nm (ε_{max} 46 433 L $mol^{-1}cm^{-1}$) (Fig. 5). Addition of aqueous solutions of Hg^{2+}, Fe^{3+} and Cu^{2+} ions (0–1.5 equiv., as ClO_4^- salts) to a solution of **10c** (30 μM in CH_3OH) resulted in the appearance of twin absorption bands at 330 and 343 nm with increased variable intensities [330 nm: ε_{max} 21 633 L mol^{-1} cm^{-1} (Hg^{2+}), 24 566 L mol^{-1} cm^{-1} (Fe^{3+}), 22 433 L mol^{-1} cm^{-1} (Cu^{2+}); 343 nm: ε_{max} 20 126 L mol^{-1} cm^{-1}(Hg^{2+}), 24 194 L mol^{-1} cm^{-1} (Fe^{3+}), 19 393 L mol^{-1} cm^{-1}(Cu^{2+})]. The high energy band at 255 nm was not perturbed significantly other than some broadening. Fitting the titration data using HypSpec, a non-linear least squares fitting programme, established the 1 : 1 stoichiometry of the most stable species present in the solution with binding constant values, log $\beta_{1,1}$ = 5.20 (Fe^{3+}), 4.69 (Hg^{2+}) and 4.45 (Cu^{2+}), respectively.

In order to understand the nature of these transitions in terms of the participation of different frontier orbitals in the observed electronic changes, we carried out TD-DFT calculations for **10c** and **10c**:M^{n+} using the Gaussian 09 suite of programs.[16] As shown in Fig. 6, we noticed that on interaction with Hg^{2+}, the HOMO (located on quinoline) was

stabilized (ΔE 0.14 eV) in comparison to **10c** and the L + 1 was raised in energy to a very small extent (ΔE 0.03 eV). This suggests that the interaction of Hg^{2+} with the quinoline part of the molecule is responsible for the quenching of the fluorescence emission. On the other hand, in the case of Cu^{2+}, the HOMO is more stabilized (ΔE 0.76 eV) as compared to **10c**:Hg^{2+} (Fig. 6), the close values of the appropriate HOMO–LUMO gap (ΔE_2, ΔE_3 and ΔE_4) corroborate the calculated binding constant values of the complexes of Hg^{2+} and Cu^{2+} with **10c**.

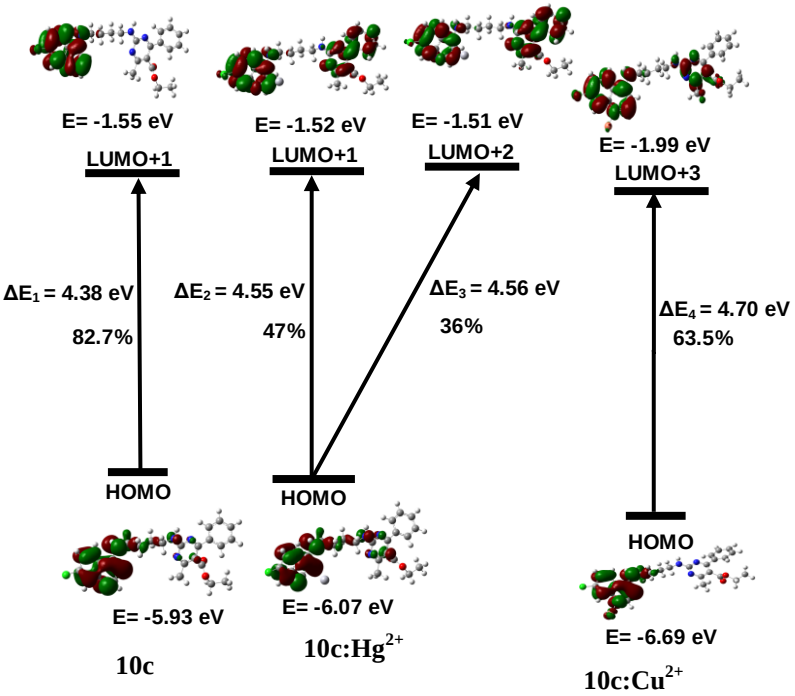

Figure 6. Energy level diagrams of HOMO (H) and LUMO (L) orbitals (isovalue 0.02) of **10c**, **10c**:Hg^{2+} and **10c**:Cu^{2+} calculated at the DFT level.

(A-4) A 'turn-off' emission based chemosensor for HSO_4^- – formation of a hydrogen-bonded complex

Further, the receptor **10c** was employed for the relatively underappreciated sensing of HSO_4^- from aqueous medium. The incremental addition of the solution of HSO_4^- (0–2.0 equiv. in H_2O) caused almost 90% emission quenching which was stabilized when the addition of one equiv. of HSO_4^- was achieved. After that no significant change was observed (Fig. 7a). The stability achieved after the addition of one

equiv. of HSO_4^- was further supported by a Job plot (a method of continuous variation) where maximum emission change was observed when the mole fraction of **10c** versus HSO_4^- was 0.5, suggesting the 1 : 1 stoichiometry for the 10c: HSO_4^- species formed in solution (Fig. 7b). The linear Stern–Volmer plot shown in Fig. 7c suggested that emission quenching arises from the static quenching process. The reason for the static quenching process may be assigned to the interaction of the fluorogenic quinoline unit of the receptor with the guest in the form of either complex formation or hydrogen bonding interactions.

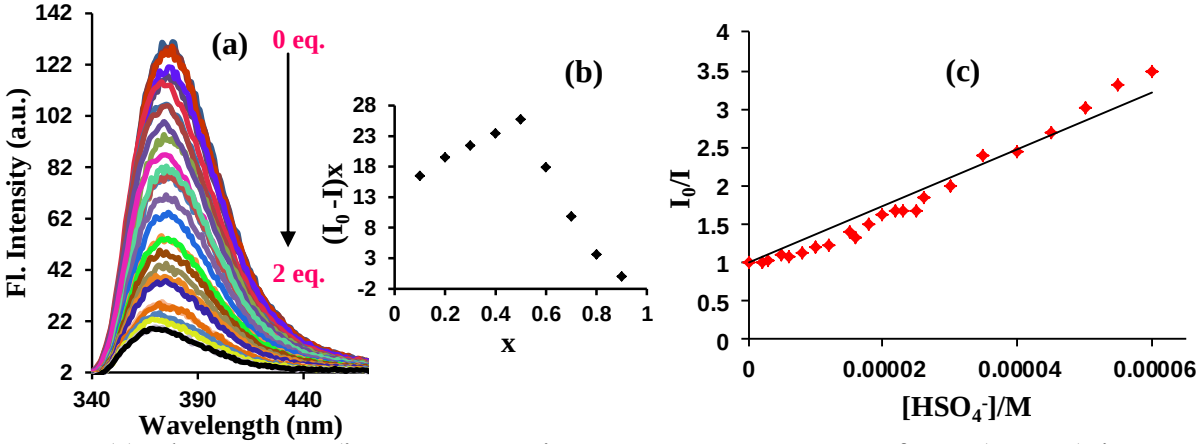

Figure 7 (a) Fluorescence (λ_{ex} = 330 nm, λ_{em} = 376 nm) spectrum of **10c** (30 μM) in CH_3OH upon addition of HSO_4^- anions (0-2 equiv.) in H_2O, (b) Job plot of HSO_4^- complex formation;

Quantum chemical calculations at the DFT level of theory are suggestive of binding of the anion through intermolecular hydrogen bonding interactions between the C-4 NH substituent and C-5 H of the quinoline moiety. As deduced from the best optimized structure (Fig. 8), the OH of HSO_4^- makes hydrogen bonding interaction with NH at the C-4 position of quinoline [N-H---O (d_{H---O} = 2.21 Å, angle NHO = 154.99°). Additionally, the O atom of HSO_4^- anion shows interaction with the quinoline C-5H (d_{O---H} = 2.77 Å, angle CHO = 104.48°) of the receptor **10c**. The role of the weak C-H---X hydrogen bonds originating from neutral system in binding the anion to the receptor finds precedence in the literature also.[17] The theoretically

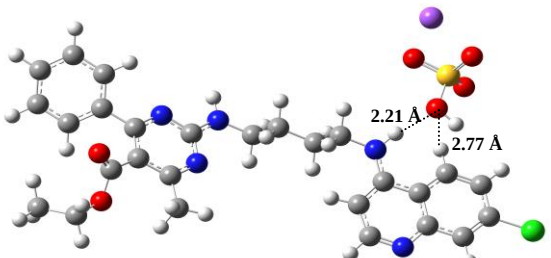

Figure 8. Calculated energy-minimized structure of **10c** with $NaHSO_4$.

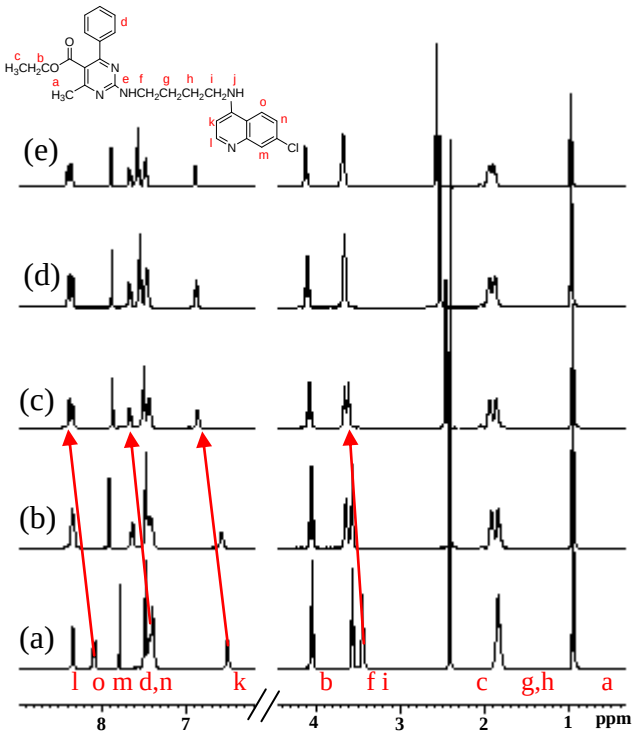

Figure 9. ^1H NMR spectral changes observed for **10c**, in CD_3OD after addition of increasing amounts of HSO_4^- anion in D_2O: (a) 0, (b) 0.50, (c) 1, (d) 1.5, and (e) 2 equiv.

predicted hydrogen bond formation between **10c** and HSO_4^- anion was further supported by the ^1H NMR titration. Gradual addition of HSO_4^- anion dissolved in D_2O was made to a solution of **10c** in CD_3OD and the ^1H NMR spectra were recorded. Considerable shift in the position of the signals involving relevant protons: H_o ($\Delta\delta$ = 0.3722 ppm), H_k ($\Delta\delta$ = 0.3394 ppm), H_n ($\Delta\delta$ = 0.2277 ppm) and H_i ($\Delta\delta$ = 0.2295 ppm) was observed (Fig. 9). The chemical shift data corroborates interaction of HSO_4^- anion as depicted in Fig. 8 and as suggested above.

Publications from this work:

1. Paramjit Kaur, Hardeep Kaur and Kamaljit Singh, *RSC Advan.*, **2013,** 3, 64-67.

2. Paramjit Kaur, Hardeep Kaur and Kamaljit Singh, *Analyst*, **2013**, 138, 425–428.

References

1. P. Biginelli, *Gazz. Chim. Ital.*, **1893**, 23, 360-416.
2. K. Singh, K. Singh, *Aust. J. Chem.*, **2008**, 61, 910-913.
3. A. Dorn, S. R. Vippagunta, H. Matile, C. Jaquet, J. L. Vennerstrom, R. G. Ridley, *Biochem. Pharmacol.*, **1998**, 55, 727-736.
4. T. J. Egan, *J. Inorg. Biochem.*, **2006**, 100, 916-926.
5. T. J. Egan, K. K. Ncokazi, *J. Inorg. Biochem.*, **2005**, 99, 1532-1539.
6. T. J. Egan, W. W. Mavuso, D. Ross, H. M. Marques, *J. Inorg. Biochem.*, **1997**, 68, 137-145.
7. J. K. Natarajan, J. N. Alumasa, K. Yearick, K. *J. Med. Chem.*, **2008**, 51, 3466-3479.
8. F. Romanelli, K. M. Smith, A. D. Hoven, *Curr. Pharm.Des.*, **2004**, 10, 2643-2648.
9. A. Savarino, J. R. Boelaert, A. Cassone, G. Majori, R. Cauda, *Lancet Infect. Dis.* **2003**, 3, 722-727.
10. (a) P. Yan, *Fluorescent Switches, Sensors, and Nanostructures*.,Vdm Verlag, **2008**; (b) P. Grundler, *Chemical Sensors. An Introduction for Scientists and Engineers*; Springer, **2008**; (c) H. N. Kim, M. H. Lee, H. J. Kim, J. S. Kim, J. Yoon, *Chem. Soc. Rev.*, **2008**, 37, 1465-1472 ; (d) C. McDonagh, C. S. Burke, B. D. MacCraith, *Chem. Rev.*, **2008**, 108, 400-422 ; (e) S. K. Kim, Lee, D. H. ; J. –I. Hong, J. Yoon, *Acc. Chem. Res.;* **2009**, 42, 23-31 ; (f) K. S. Johnson, J. A. Needoba, S. C. Riser, W. J. Showers, *Chem. Rev.;* **2007**, 107, 623-640.
11. J. F. Callan, A. P. de Silva, D. C. Magri, *Tetrahedron* **2005**, 61, 8551-8588.
12. (a) H. Zheng, M. Yan, X. -X. Fan, D. Sun, S.-Y. Yang, L.-J. Yang, J. -D. Li, Y.-B. Jiang, *Chem. Commun.*, **2012**, 48, 2243–2245; (b) L. Huang, J. Cheng, K. Xie, P. Xi, F. Hou, Z. Li, G. Xie, Y. Shi, H. Liu, D. Bai, Z. Zeng, *Dalton Trans.*, **2011**, 40, 10815–10817; (c) H. S. Jung, P. S. Kwon, J. W. Lee, J. Kim, C. S. Hong, J. W. Kim, S. Yan, J. Y. Lee, J. H. Lee, T. Joo, J. S. Kim, *J. Am. Chem. Soc.*, **2009**, 131, 2008–2012; (d) S.

Voutsadaki, G. K. Tsikalas, E. Klontzas, G. E. Froudaskis, H. E. Katerinopoulos, *Chem. Commun.*, **2010**, 46, 3292–3294; (e) M. Hu, J. Fan, J. Cao, K. Song, H. Zhang, S. Sun, X. Peng, *Analyst*, **2012**, 137, 2107-2111; (f) J. Yao, W. Dou, W. Qin, W. Liu, *Inorg. Chem. Commun.*, **2009**, 12, 116–118; (g) D. -N. Lee, G. -J. Kim, H. -J. Kim, *Tetrahedron Lett.*, **2009**, 50, 4766–4768.

13. (a) F. Hou, J. Cheng, P. Xi, F. Chen, L. Huang, G. Xie, Y. Shi, H. Liu, D. Bai, Z. Zeng, *Dalton Trans.*, **2012**, 41, 5799–5804; (b) M. Li, H. -Y. Lu, R. -L. Liu, J. -D. Chen, C. -F. Chen, *J. Org. Chem.*, **2012**, 77, 3670–3673; (c) A. -B. Bon, A. M. Costero, S. Gil, M. Parra, J. Soto, R. Martinez-Manez, F. Sancenon, Chem. *Commun.*, **2012**, 48, 8407; (d) X. Zeng, L. Dong, C. Wu, L. Mu, S. Xue, Z. Tau, *Sens. Actuators, B*, **2009**, 141, 506–510; (e) A. K. Mandal, M. Suresh, E. Suresh, S. K. Mishra, S. Mishra, A. Das, *Sens. Actuators, B*, **2010**, 145, 32–38; (f) B. N. Ahamed, I. Ravikumar, P. Ghosh, *New J. Chem.*, **2009**, 33, 1825–1828; (g) S. Ghosh, R. Chakarbarty, P. S. Mukherjee, *Inorg. Chem.*, **2009**, 48, 549–556.

14. (a) Z. Xu, K. -H. Baek, H. N. Kim, J. Cui, X. Quan, D. R. Spring, I. Shin, J. Yoon, *J. Am. Chem. Soc.*, **2010**, 132, 601–610; (b) Q. Li, M. Peng, H. Li, C. Zhong, L. Zhang, X. Cheng, X. Peng, Q. Wang, J. Qin, Z. Li, *Org. Lett.*, **2012**, 14, 2094–2097; (c) H. Zheng, X. -J. Zhang, X. Cai, Q. -N. Bian, M. Yan, G. -H. Wu, X. W. Lai, Y. -B. Jiang, *Org. Lett.*, **2012**, 14, 1986–1989; (d) X. Qu, Q. Liu, X. Ji, H. Chen, Z. Zhou, Z. Shen, *Chem. Commun.*, **2012**, 48, 4600–4602.

15. (a) W. Xuan, C. Chen, Y. Cao, W. He, W. Jiang, K. Liu, W. Wang, *Chem. Commun.*, **2012**, 48, 7292–7294; (b) S. Kotha, D. Goyal, S. Banerjee, A. Datta, *Analyst*, **2012**, 137, 2871–2875; (c) X. Sun, Y.-W. Wang, Y. Peng, *Org. Lett.*, **2012**, 14, 3420–3423; (d) X. Wang, J. Hu, T. Liu, G. Zhang, S. Liu, *J. Mater. Chem.*, **2012**, 22, 8622–8628.

16. M. J. Frisch et al., Gaussian 09, Revision B.01, Gaussian, Inc.,Wallingford, CT, **2010.**

17. (a) G. R. Desiraju, *Acc. Chem. Res.*, **2002**, 35, 565–573; (b) V. S. Bryantsev, B. P. Hay, *J. Am. Chem. Soc.*, **2005**, 127, 8282–8283.

List of publications from this project:

1. Kamaljit Singh, Hardeep Kaur, Kelly Chibale, Jan Balzarini, Susan Little, Prasad V. Bharatam, *Eur. J. Med. Chem.*, **2011**, 52, 82-97.

2. Kamaljit Singh, Kawaljit Singh, Danielle M. Trappanese, Robert S. Moreland, *Eur. J. Med. Chem.*, **2012**, 54, 397-402.
3. Kamaljit Singh, Kawaljit Singh, Baojie Wan, Scott Franzblau, Kelly Chibale and Jan Balzarini, *Eur. J. Med. Chem.*, **2012**, 46, 2290-2294.

(iii) Has the progress been according to original plan of work and towards achieving the objective. If not, state reasons : The progress has been according to the original plan of work and the objectives have by and large been achieved.

(iv) Please indicate the difficulties, if any, experienced in implementing the Project: Nil

(v) If project has not been completed, please indicate the approximate time by which it is likely to be completed. A summary of the work done for the period (Annual basis) may please be sent to the Commission on a separate sheet : The project is completed and the report is provided.

(vi) If the project has been completed, please enclose a summary of the findings of the study. Two bound copies of the final report of work done may also be sent to the Commission.

(A) 2-Aminopyrimidine based 4-aminoquinoline anti-plasmodial agents have been synthesized and their activity and its relationship with structure has been established.

(B) Highly regioselective synthesis of N-3 organophosphorous derivatives of 3,4-dihydropyrimidine-2(1*H*)-ones and their calcium channel binding studies have been established.

(C) Facile transformation of Biginelli pyrimdin-2(1*H*)-ones to pyrimidines has been achieved. *In vitro* evaluation revealed these compounds to be potent anti-mycobacterial agents as well as modulators of cytotoxicity.

(vii). Any other information which would help in evaluation of work done on the project. At the completion of the project, the first report should indicate the output, such as (a) Manpower trained (b) Ph. D. awarded (c) Publication of results (d) other impact, if any:

Results have been published in international journals of repute and the list is attached. Further, two Ph.D. students got training in this project, although they had open fellowships of UGC and CSIR.

SIGNATURE OF THE PRINCIPAL INVESTIGATOR **REGISTRAR/PRINCIPAL**